Nano Hybrids
ISSN: 2234-9871, Vol. 4, pp 61-85
doi:10.4028/www.scientific.net/NH.4.61
© 2013 The Author(s). Published by Trans Tech Publications Ltd, Switzerland.
Online: 2013-05-24

Synthesis, Characterization, Modeling and Anti-bacterial Properties of Peanut-shaped ZnO Nano-bunches

Mohd Farhan Khan*[1,2,a], Akhter H. Ansari[1,b], M. Hameedullah[1,c], M. B. Lohani[2,d], Mohammad Mezbaul Alam*[3,e], Zeid A. AlOthman[3,f], Abu Mustafa Khan[4,g] and Mohd. Kamran Khan[5,h]

[1]Nanosolver Laboratory, Department of Mechanical Engineering, Zakir Hussain College of Engineering & Technology, Aligarh Muslim University, Aligarh 202 002, India.

[2]Department of Applied Chemistry, Integral University, Lucknow 226 026, India.

[3]Advanced Materials Research Chair, Chemistry Department, College of Science, Building 5, King Saud University, Riyadh, Kingdom of Saudi Arabia.

[4]Department of Chemical Engineering, Zakir Hussain College of Engineering & Technology, Aligarh Muslim University, Aligarh 202 002, India.

[5]Hematopathology Lab, Prince Faisal Cancer Center, Buraida, Kingdom of Saudi Arabia.

(*Corresponding Autohor) *[a]nanotailorgroup@gmail.com, [b]ahaansari@yahoo.com, [c]hameedullah_amu@yahoo.com, [d]minaxilohani@gmail.com, *[e]dr.mezbah1974@gmail.com, [f]zaothman@ksu.edu.sa, [g]mmustafa066@gmail.com, [h]kamran_khan865@yahoo.com

Keywords: Peanut-shaped ZnO nano-bunches, $C_{19}H_{42}NBr$ complex, Modelling and simulation, Anti-bacterial activity, *Bacillus subtilis.*

Abstract. Since few decades, the fabrications of metal oxide nanoparticles (MO-Nps) as well as their uses in various segments have been increased manifolds. An easy effort to produce an important category of MO-Nps as Zinc oxide nano-particles (ZnO-Nps), with the assistance of *mechano-solution method* at various low temperatures, introducing Zinc acetate dihydrate and Sodium hydroxide into the molar solution of $C_{19}H_{42}NBr$ complex (Cetrimonium bromide, CTAB) for much less than an hour was projected. The impact of this method performed at two different ranges of process temperatures was studied and the magnitude of the ZnO-Nps (like

This article is an open access article under the terms and conditions of the Creative Commons Attribution (CC BY) license
(https://creativecommons.org/licenses/by/4.0)

particle size, morphology and L/D dimensions) has been reported. On the top of this, the morphological study of these Nps has been presented. The characterization of the synthesized Nps was carried out with the help of SEM with EDS, XRD, UV-Vis spectroscopy. The scanning electron microscopy has revealed the synthesis of peanut-shaped ZnO nano-bunches (NBs) at two different ranges of temperature. An overall viable growth of the solitary nano-particles constituting of ZnO-NBs has also been put forth. Hence, the effect of temperature on $C_{19}H_{42}NBr$ complex (stabilizer) has been reported. In addition, a postulated model depicting the relationship of the temperature effect on the process parameters of ZnO-NBs has also been floated. The Gram +ve bacteria, *Bacillus subtilis* is a rod shaped bacteria which is commonly known as normal gut commensal in humans. Due to the emergence of anti-biotic resistant drugs, alternate medications are under primary considerations. A noteworthy experimentation was concerned with anti-bacterial activity of therapeutically viable Gram +ve bacteria, *Bacillus subtilis* and it was found that reported ZnO-NBs have become the promising entities for terminating the growth of these bacterias.

Introduction

Zinc oxide (ZnO) is an important n-type semi-conducting metal oxide with a band gap of about 3.3 eV at 300 K and a large exciton B.E. at 298 K of 60 meV. It also reveals p-type conduction property, when doped with other transition metals [1,2]. It has also shown its competence for various types of dermatological ailments. Due to this, they are more efficiently used as sunscreens, photocatalysts, cosmetics and in a variety of therapeutic formulations as it is treated for potential interventions in extrinsic skin problems like aging, sunburn, etc. Besides these, ZnO-Nps showed strange effect as an UV-absorber when treated on the external surface of cotton and woollen fabrics [3–6]. Thre are various synthesis procedures for ZnO-Nps, such as sol-gel technique, facile biomimetic process, mechanochemical process, solvothermal process, solution method, etc. These processes lead to various types of morphological arrays of ZnO-Nps and in continuation leads to the diversified range of their application based upon their morphologies [7–12]. The various types of

process parameters viz. temperature, concentration of reacting species, time, pH, doping, etc; used in different techniques and processes decide the morphology, particle size, yield, properties and diverse applications of the synthesized ZnO-Nps. More complex techniques also lead to the increase in the total cost of the synthesis. Worldwide, many researchers developed a large number of techniques to control of these process parameters [13–18].

Formerly, Wahab et al. [7] in one of their experiments, has developed an aged pencil like Zinc oxide nano-rods by solution method, where they refluxed the solution at 75 °C for different time intervals; in his other paper, he presented the plate-like to flower-like morphology of ZnO nanostructures by varying pH of precursor solution and refluxing the whole solution at 90 °C for an hour [13]. Again in his next study, he presented the synthesis of single-crystalline needle-shaped ZnO nanorods via sonochemical method, where he performed the sonication of the solution on sonication bath for 2-4 hrs [20]. Gan et al. [8] synthesized peanut-like and flower-like Zinc oxide 3D architectures by a facile biomimetic process using gelatin as matrix after keeping the suspension at 30 °C for 24 hrs and centrifuged for 12 hrs. Mclaren et al. [12] modified technique of Andelman et al. and developed the ZnO nanorods. Qin et al. [19] fabricated ZnO nanowire arrays and ZnO nanoparticles electrodes at 95 ^{o}C for 24 hrs. Teki et al. [21] demonstrated ZnO nanorods growth on Si(100) wafers by magnetron sputtering at temperatures less than 100 °C, with a power of 100W and 0.16 Pa Ar working pressure. In concise, the synthesis of ZnO-Nps at near ambient temperatures was required, keeping the consideration of nano-particles sizes, their L/D ratios and definitely the morphology of ZnO-Nps, by preventing the expensive and complicated systems to be utilized for various low temperature UV appealing medications and devices. An earlier reported approach by our team involves low temperature, below the boiling point of water and avoids sophisticated equipments for the production of ZnO-Nps [22]. Comparing with all the techniques for the fabrication of ZnO-Nps, the mechano-solution method is economical, less-time consuming and after all, an easy process.

In this work, the simple mechano-solution synthesis of peanut-shaped ZnO nano-bunches (ZnO-NBs) and flower-shaped ZnO-NPs, at near ambient temperatures (viz. 40±3 and 60±3 °C) using Zinc acetate diyhdrate and sodium hydroxide (NaOH) in the presence of the cationic surfactant hexadecyltrimethylammonium bromide (CTAB) ($C_{19}H_{42}NBr$) complex has been reported. Along with the simple mechano-solution method, responsible for the synthesis of ZnO-NBs, different results of characterization techniques like XRD, SEM with EDS and UV-Vis spectroscopy have been discussed; the effect of different temperature conditions on the crystallite size, pH, L/D ratios, morphology of the nano-bunches as well as an easy growth mechanism have also been presented. In the last, the relationship of the changing temperature condition and the different aspect-ratios of ZnO nano-bunches have been presented with a help of a suitable model. From the literature, the studies revealed that the nanoscaled ZnO particles were more toxic to all bacterial species than other nanoparticles of different inorganic oxides like aluminium oxide, silicon dioxide, etc [23–26]. Finally, the anti-bacterial activity of synthesized ZnO-NBs were tested against Gram +ve bacteria, *B. subtilis* (MTCC 121). Though *B. subtilis* is not as much harmful as other pathogenic bacterias, but it is an easy model for doing the clinical studies and checking the anti-bacterial activity as the mechanism for attacking on the Gram +ve bacterial colonies are same.

Experimentation

Materials. All the reaction species viz. Zinc acetate dihydrate, Ion-carrier Sodium hydroxide and the capping agent hexadecyltrimethylammonium bromide (CTAB) ($C_{19}H_{42}NBr$) complex were taken of analytical grade and purchased from E. Merck Ltd. (Mumbai, India) and Loba (Mumbai, India) respectively and used without any further purification.

Fabrication of Zinc oxide nano-bunches (ZnO-NBs). The synthesis of ZnO-NBs was performed by the mechano-solution method. The mixed solutions of capping agent CTAB and Zinc acetate dihydrate, prepared in a DD water were thoroughly stirred. In to this required amount of NaOH was added gradually. The amount of Zinc acetate dihydrate, CTAB and NaOH were taken as 0.1 gm, 2 gm and 0.2 gm, respectively. After a span of minutes, the round bottom flask kept on a steady temperature operation tool showed the appearance of an opaque milky like liquid with an upper thick foamy layer. When it reached to room temperature, the colloidal suspensions so formed was kept under refrigeration for a while and then stored for the characterization.

Characterization of ZnO-NBs. The X-ray diffraction patern of the prepared ZnO nanocolloidal were investigated by a BRUKER AXD D8 ADVANCE (Germany) X-ray diffractometer, using X-ray beam with nickel filtered CuKα radiations of wavelength equal to 1.54 Å and with a step dimension of 0.01° and scanning speed of 0.02 steps/second. A fixed power generation of 40 kV and 40 mA was used. The nanoparticulate sizes were further calculated with the help of spectral peaks by Debye-Scherer formula [27,28]:

$$D = \frac{k\lambda}{\beta \cos\theta}$$

where, D = Crystallite size, k = proportionality constant (0.9), λ = X-ray wavelength (1.54178 Å), β = FWHM of XRD peaks and θ = Braggs' angle

The calculation was further simplified by the integrated software, Diffrac^{plus}. The UV-Vis absorption spectroscopy was performed by double beam PERKIN-ELMER Spetrophotometer. The DD water was used as a reference for background correction [6]. The morphological aspect (shape and D/L values) were recorded with the help of Scanning electron microscopy, JEOL JSM-6510 LV (Japan) [29]. The TEM images of peanut-shaped ZnO 1D Single crystals have been taken from an advanced version of Field emission electron microscope with model no. JEM-2100F. It gives the performance of the 200kV class along with the probe size under 0.5 nm.

Anti-bacterial Activity of ZnO-NBs. For anti-microbial activities were studied by Disc diffusion method with the help of nutrient agar along with suspended microbes, by dipping the pad into the culture. After streaking the agar plate, these are incubated for 24 hrs. Antibiotic discs were kept on agar surfaces and the anti-bacterial activities were noted from the inhibition zones (IZ) results and finally the calculation of diameters of IZ of stains were carried out. The ZnO Nano-bunches (ZnO-NBs) fabricated at different temperature ranges were taken and their colloidal suspensions were tested for their activity against *Bacillus subtilis*. For this purpose the filter paper disc technique was exploited. Prior to this, the ZnO-NBs were attempted with bactericidal activity by disc diffusion method for *Bacillus subtilis*. The cultures used were kept over night at 37 °C on nutrient agar. On preceding the process, the cultures were centrifuged at moderate rpm range and the pellets were diluted in NSS to get the count more than 100 cfu/ ml. The bacterial culture suspension was extended on the plates of Nutrient agar homogeneously and 8 mm discs of Hi-media Pvt Ltd make were made sterile for ZnO-NBs. These plates were further kept at 37 °C for another day. Standard anti-biotic discs of 0.03 mg each and doxycycline were utilized and ZnO-NBs media of similar concentrations were set as control. Later the resulting inhibition zones (IZ), in mm of bacterial growth were calculated for the determination of anti-bacterial activities [30,31].

Result and Discussion

The Zinc oxide nano-bunches (ZnO-NBs) formed at two different ranges of temperature showed reasonable effects on particle sizes, shape and the L/D ratios of fabricated ZnO-NBs. The two temperature ranges were shown in Table 1, as TEMP-I (40±3 °C) and TEMP-II (60±3 °C).

Table 1. The effect of various reaction conditions at different temperature ranges; TEMP-I and TEMP-II, on the synthesis and characteristics of Peanut-shaped ZnO-NBs

Sample	Crystallite size (nm)	Maximum absorbance (nm)	Length of Peanut-shaped ZnO L (nm)	Width of Peanut-shaped ZnO D (nm)	Aspect-ratio of Peanut-shaped ZnO (L/D)
Peanut-shaped ZnO-NBs (40±3°C) TEMP-I	80.38	296	362	93	3.89
Peanut-shaped ZnO-NBs (60±3°C) TEMP-II	66.25	295	790	375	2

XRD Analysis of ZnO-NBs. The X-ray diffraction pattern of ZnO-NBs (TEMP-I & TEMP-II) prepared at different temperature ranges were examined (Fig. 1). One-dimentional single crystals of ZnO-NBs showed different sizes in the two temperature ranges. The values of the indices were in accordance with the ICDD data. The XRD results showed that by changing the process temperature ranges, the average particle size of the ZnO-NBs changes. The diameter of the one-dimentional (1D) single crystal of the ZnO-NBs showed a considerable shift along with the temperature variation in the experimental process. On decreasing the process temperature, the diameter of the one-dimentional (1D) single crystal of the ZnO-NBs decreases. Similarly, the length of the 1D single crystal also decreases with decrease in process temperature range. Wahab et al. [7] reported pencil-like Zinc oxide nanostructures at a reflux temperature of 75 °C for different time intervals i.e 12 h, 24 h, 36 h, 48 h, 60 h and concluded that the thickness and length of the pencil-like zinc oxide nanostructure increases when the refluxing time of Zinc acetate di-hydrate and Sodium hydroxide solution increases [7].

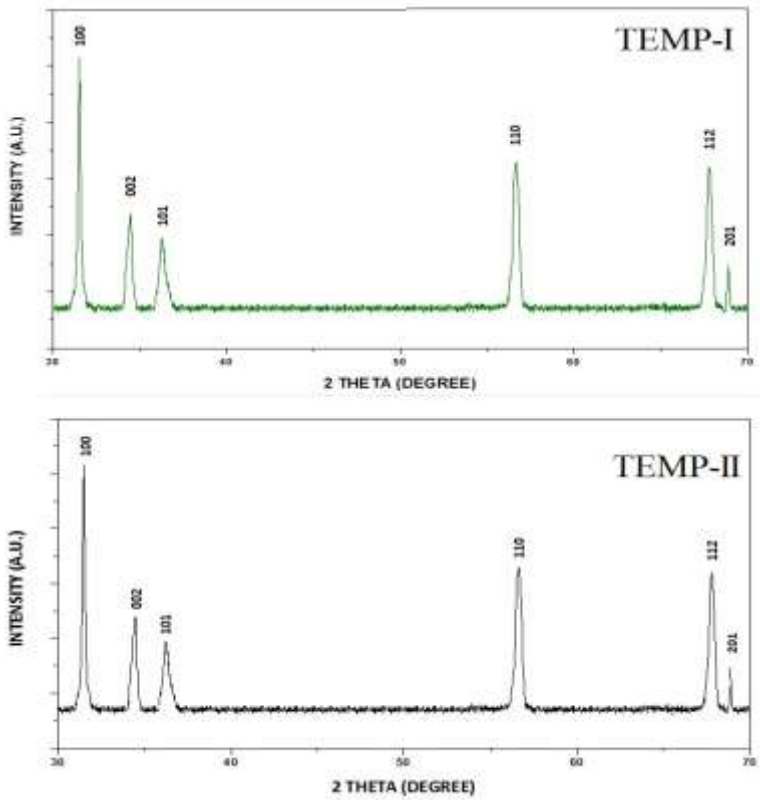

Fig. 1. XRD of Peanut-shaped ZnO-NBs prepared at different temperature ranges; TEMP-I (40±3°C) and TEMP-II (60±3°C).

UV-vis spectroscopy of ZnO-NBs. The double beam UV-Vis spectrophotometer was used for the optical characterization of the samples. The absorbance peak was shown are higher for TEMP-I range as compared to TEMP-II range (Fig. 2). The earlier literature showed the peak shift dependency on crystallite size, process temperature, synthesis method and samples aging [32]. The results were in agreement with that of Guan et al. [33].

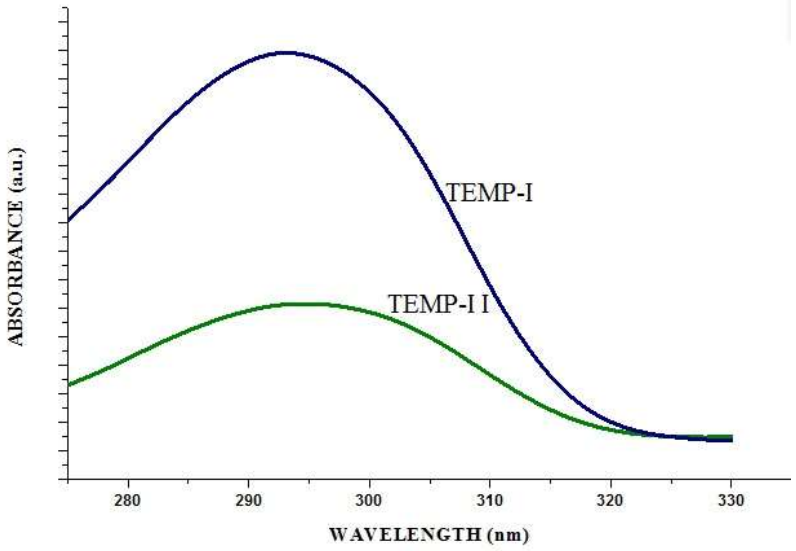

Fig. 2. UV-vis spectra of Peanut-shaped ZnO-NBs prepared at different temperature ranges; TEMP-I and TEMP-II.

Morphology of ZnO-NBs. From the SEM images, existence of one-dimensional (ID) single crystal ZnO nano-bunches is revealed. On lowering the process temperature range, the Nano-bunch size as well length and diameter of the Peanut shaped ID single crystal also decreases. The magnified morphology of the 1D ZnO single crystals showed the appearance of a Peanut form of crystal. But it seems that the Peanut-shape may finally lead to Rod-shape 1D single crystal, when the processing temperature range was reduced, in this particular type of fabrication process, namely Mechno-solution Technique (Fig. 3,4). Gan et al. [8] presented two types of 3D ZnO architecture: one was the peanut-like and other was the flower-like structures. The peanut-like fabrications were obtained when used the concentration of Zn^{2+} as 0.06 mol/L. The results showed the abundance of an array of ZnO nano-bunches comprising of Peanut-shaped one-dimensional (1D) single crystals.

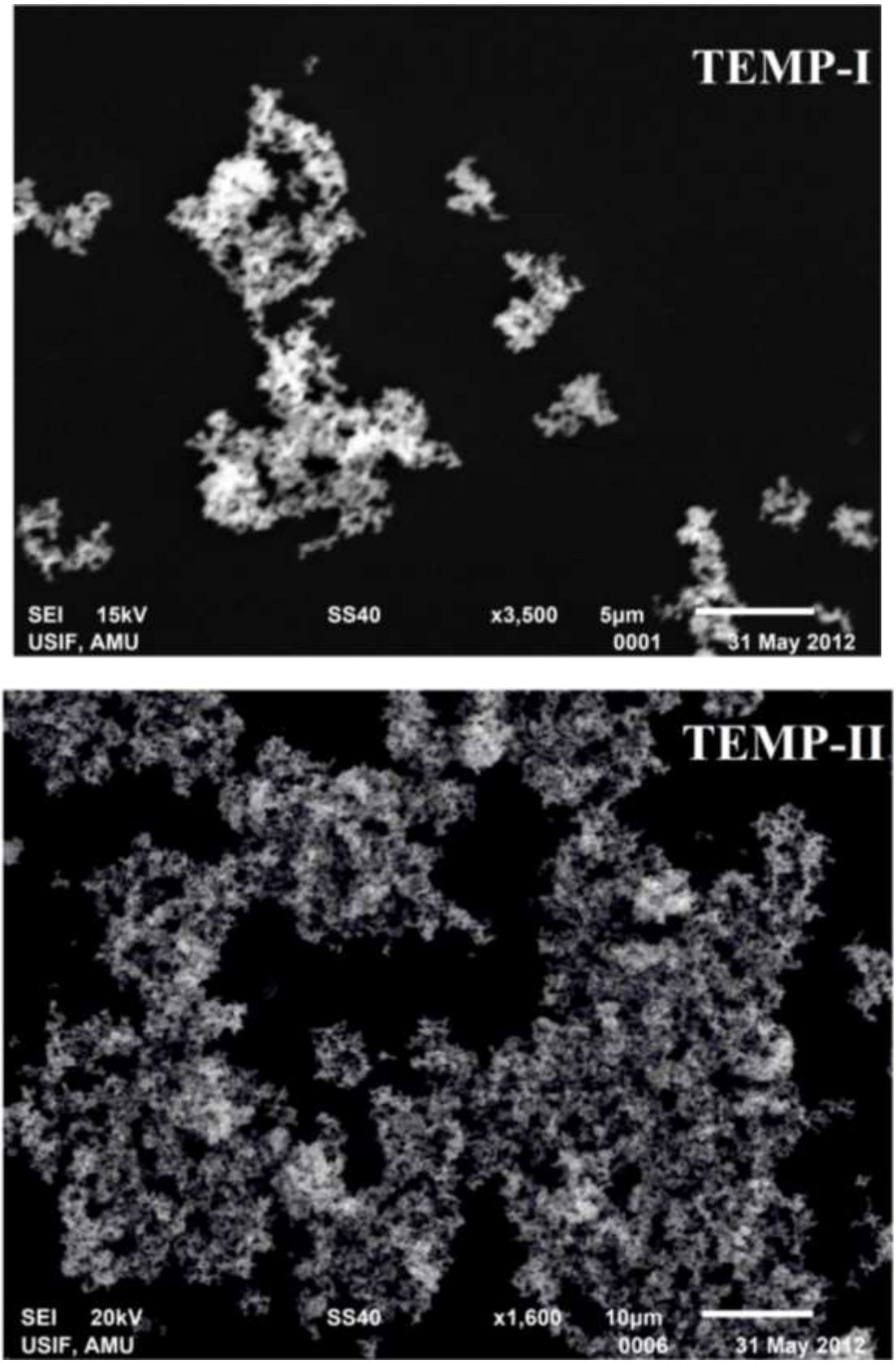

Fig. 3. SEM photographs of Peanut-shaped ZnO-NB prepared at different temperature ranges; TEMP-I and TEMP-II.

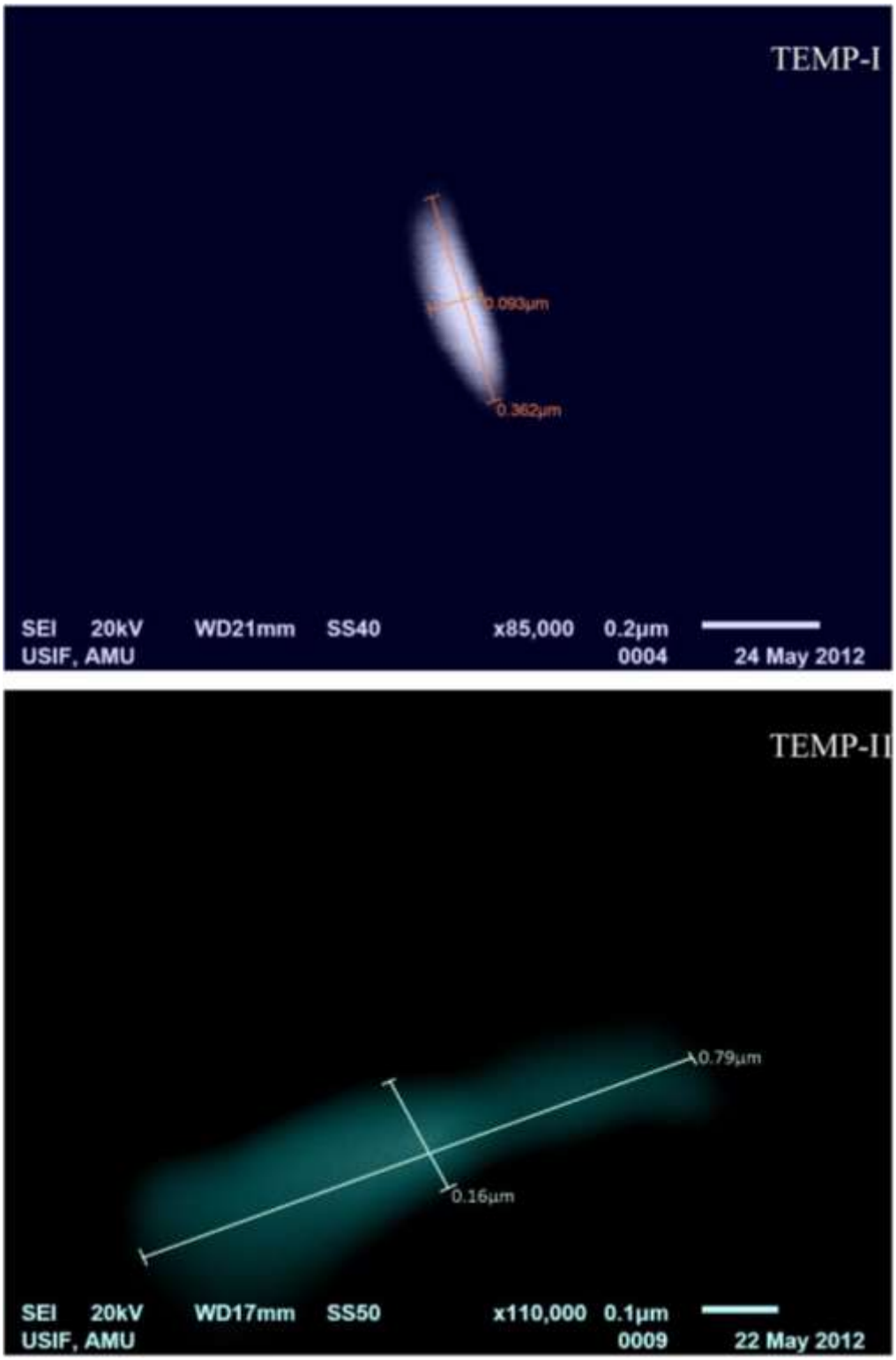

Fig. 4. SEM photographs of Peanut shaped ZnO 1D Single crystal prepared at different temperature ranges; TEMP-I and TEMP-II.

EDAX of ZnO-NB. The EDAX spectrum of the Peanut-shaped ZnO nano-bunches were shown in Fig. 5. The prior one was for the temperature range TEMP-I and the latter one for TEMP-II, which were told in the beginning of this part. In the spectrum, Zn and O spectras were important.

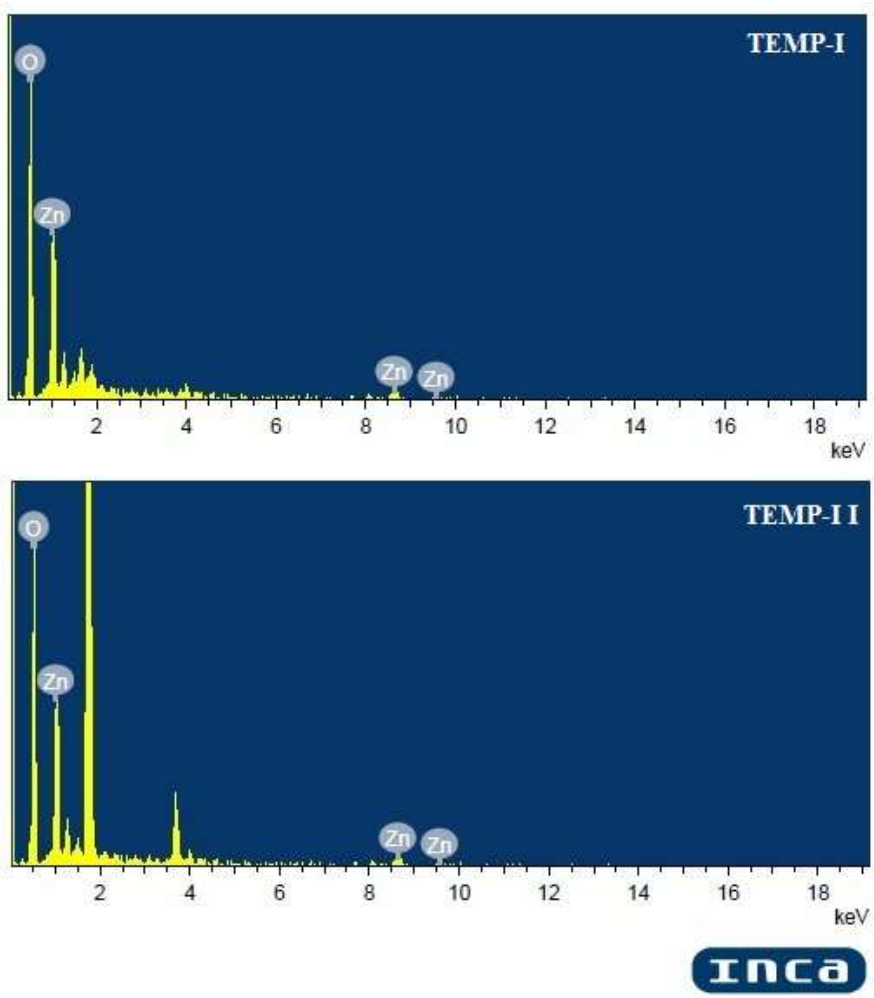

Fig. 5. EDAX of Peanut-shaped ZnO-NBs prepared at different temperature ranges; TEMP-I and TEMP-II.

From the TEM images (Fig. 6), the existence of one-dimensional (1D) single crystal ZnO nano-bunches has been validated. The magnified images of both the samples, clearly signifies the claimed shape of nano-Zinc oxides, which are consistent with the SEM results. The SAED pattern (inset) also shows the diffraction patterns, which relates the results for ZnOone-dimensional (1D) single crystal structure. Gan et al. [8] also presented the HRTEM images of the peanut-like ZnO sample which are consistent in the FESEM observations.

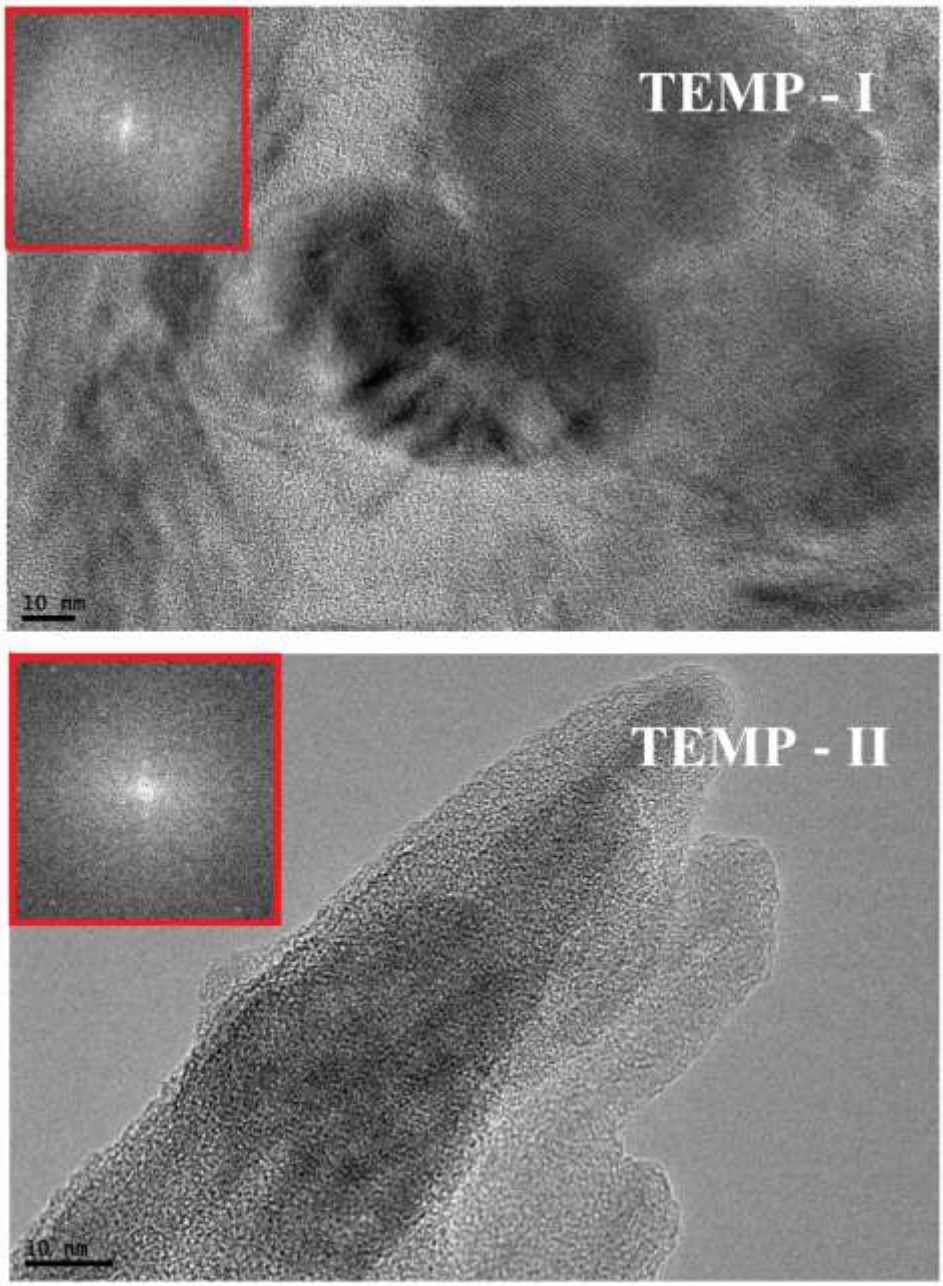

Fig. 6. TEM images along with SAED patterns (inset) of Peanut shaped ZnO 1D Single crystal prepared at different temperature ranges; TEMP-I and TEMP-II.

L/D Ratios of ZnO-NBs. From the SEM images, this was revealed that calculated length & diameter values of the objected L/D ratios [34] of peanut-shaped 1D single crystals were also attributed with the nature of process temperature change. At lower temperature, the L/D value increases (Fig. 7,8,10). This is due to the fact that on decreasing the temperatue, both the length and

the diameter of the NB decreases, but the proportion of reduction of the diameter (D) was much more as compared to the length (L) of the peanut-shaped ZnO nano-bunches in the samples TEMP-I. This all ultimately leads to the formation of Peanut-shaped ZnO to Rod-shaped ZnO (on coming more down the process temperature line).

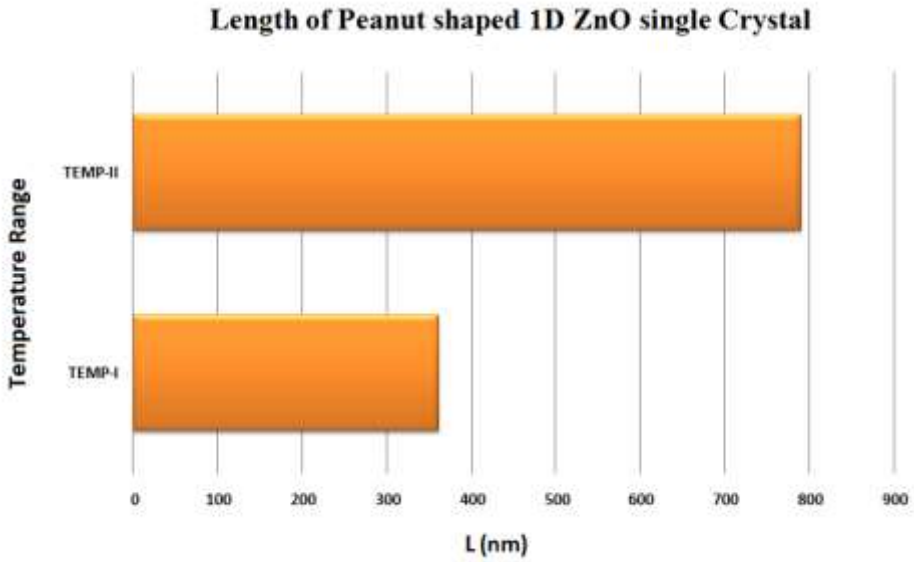

Fig. 7. Comparative chart of Length (L) of Peanut-shaped 1D-ZnO single crystal prepared at different temperature ranges; TEMP-I and TEMP-II.

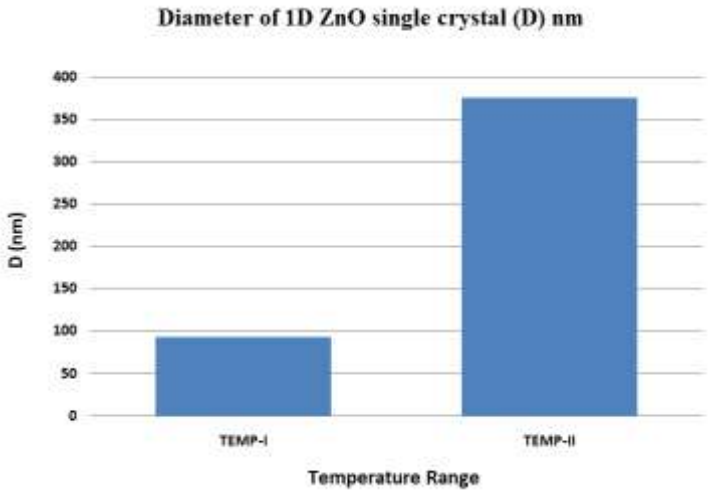

Fig. 8. Comparative chart of Diameter (D) of Peanut-shaped 1D-ZnO single crystal prepared at different temperature ranges; TEMP-I and TEMP-II.

Growth Mechanism of ZnO-NB

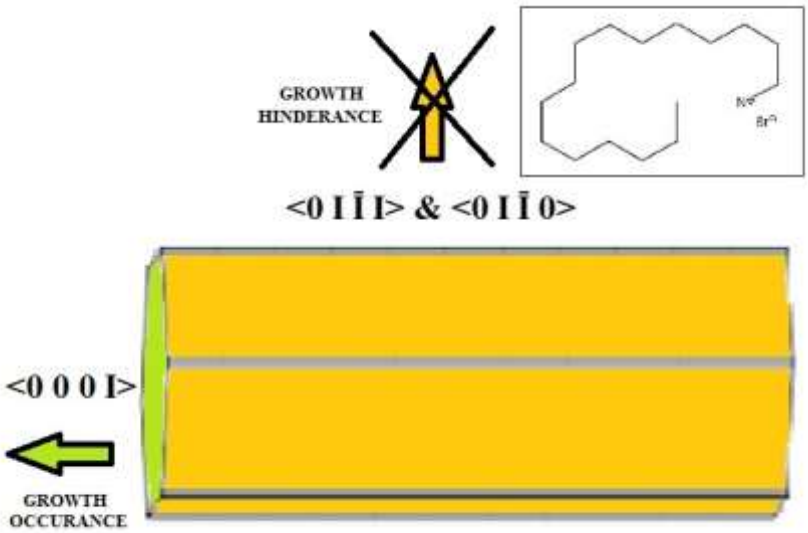

Fig. 9. Schematic representation of the growth order of the Peanut shaped one-dimensional (1D) single crystal ZnO (in the presence of $C_{19}H_{42}NBr$).

Here the growth of ZnO nano bunches along the direction of <0 0 0 1> axis, resulting into a bunch of one-dimensional single crystals. As per the observed results, the *L/D ratios* of the Peanut shaped 1D single crystals of ZnO NB at two different temperature ranges showed as (Fig. 7-10):

$$\boldsymbol{L}^{\text{TEMP-I}} > \boldsymbol{L}^{\text{TEMP-II}} \quad (1)$$

$$\boldsymbol{D}^{\text{TEMP-I}} > \boldsymbol{D}^{\text{TEMP-II}} \quad (2)$$

$$\boldsymbol{L/D}^{\text{TEMP-I}} < \boldsymbol{L/D}^{\text{TEMP-II}} \quad (3)$$

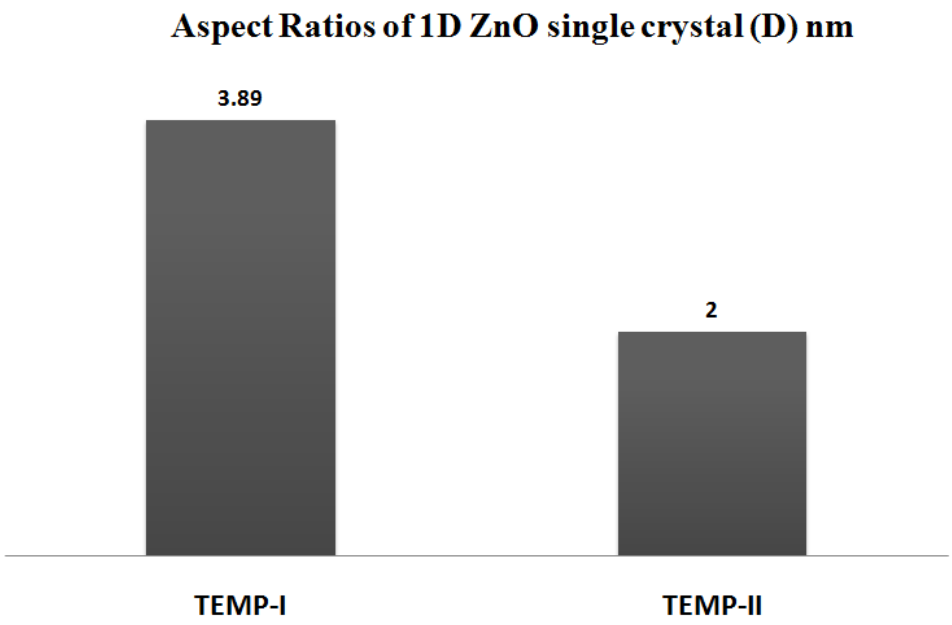

Fig. 10. Comparative chart of Aspect Ratio (L/D) of Peanut-shaped 1D-ZnO single crystal prepared at different temperature ranges; TEMP-I and TEMP-II.

The presence of $C_{19}H_{42}NBr$ complex (stabilizer) that binds more towards the faces <0 I Ī I> & <0 I Ī 0>, changes the free energy and slows the growth of these faces [12]. In both the temperature ranges i.e TEMP-I & TEMP-II, the length and diameter were decreased on lowering the temperature. But still the aspect-ratio was increased notably. This was due to the fact that on lowering the temperature or moving from TEMP-II to TEMP-I, the growth of face <0 0 0 I> hinders but not as much as of faces <0 I Ī I> & <0 I Ī 0>, where on lowering the temperature, the action of $C_{19}H_{42}NBr$ complex increased in binding on faces <0 I Ī I> & <0 I Ī 0> and this slows the growth of these faces, by changing the free energy. Hence this showed the effect of temperature on $C_{19}H_{42}NBr$ complex (stabilizer). This all leads to the one-dimensional single crystal enhancement of L/D ratio.

Modeling and Simulation of ZnO-NBs. In research works, only data is of no importance unless until one would able to get some useful result from it. And it is not only a trend one predicts in a data. The data becomes very important and useful if someone able to give a relation based on it. Here the modelling comes into picture. By using various mathematical tools modelling was done. In our

work, we used a very simple and old technique to develop a model of change in aspect ratio with change in temperature. Least square method was used to develop the model which comes out to be a straight line with slope 0.094 decreasing and intercept 7.67 that is

$$y = -0.094x + 7.67$$

It shows a decreasing trend in aspect ratio with increasing temperature. Other things were explained in result and discussion section. We chose least square method because of easiness and reliability. It is a very old but reliable technique. Least square method is used for developing the model for change in aspect ratio with temperature. The following equations are required:

$$\sum y = na + b \sum x \quad (4)$$

$$\sum xy = a \sum x + b \sum x^2 \quad (5)$$

For these equations following table (Table 2) was used:

Table 2. Calculation table for the development of model depicting the relationship between L/D ratios of Peanut-shaped ZnO-NBs formed at different temperature ranges.

X	Y	XY	X^2
TEMP	(L/D)		
Peanut-shaped ZnO-NBs (40±3°C) TEMP-I	3.89	155.6	1600
Peanut-shaped ZnO-NBs (60±3°C) TEMP-II	2	120	3600
∑ 100	5.89	275.6	5200

By using Table 2, we got the equations written above as follows:

$$5.89 = 2a + 100b \quad (4')$$

$$275.6 = 100a + 5200b \quad (5')$$

Solving these equations, we got the values of a and b as: a = 7.67, b = -0.094.

Now the model required is:

$y = -0.094\,x + 7.67$

ZnO-NBs as Anti-Bacterial Agents. The influence of metal oxide nano-particulates (MO-Nps) with the pathogenic bacterias is an evolving area for research. Consequently, after fruitful characterization results, the peanut shaped ZnO nano-bunches fabricated at different temperature range were tested for their bactericidal performances. The different proportions of ZnO nano-bunches exhibited significantly anti-bacterial activity against the Gram +ve bacteria, *Bacillus subtilis,* responsible for producing the heat stable toxin amylopsin related to food borne illness. The concentration dependent anti-bacterial activity shown in terms of zone of inhibition was visible on NA plates (Fig.11). At highest concentration, the growth of bacterial strains, *Bacillus subtilis* was stop down appreciably (Table 3).

At 500 μg/ml of Peanut shaped ZnO nano-bunches, maximum zone of inhibition (IZ) i.e. 22 mm was recorded for *B. subtilis* (MTCC 121) by ZnO-NBs fabricated at TEMP-II. After that the maximum zone of inhibition (IZ) of about 20 mm was recorded for *B. subtilis* (MTCC 121) by Peanut-shaped ZnO nano-bunches fabricated at TEMP-I. The initial readings also postulate that the anti-bacterial performances of ZnO-NBs may be dependent of size & morphology of peanut-shaped ZnO-NBs. The bactericidal properties of these peanut shaped ZnO-NBs recommend that these nano-bunches were more diffusible in the growth culture medium which allows the superior interferences among bacterial cells and that of nano-bunches. Similar anti-bactericidal impacts of some other ZnO nano-particles fabricated from other techniques are also known [35-37]. The stains of Gram+ bacteria, *Bacillus subtilis,* were most vulnerable to the ZnO nano-particulates. This might be due to presences of some proteins and polysaccharides on surface of cell wall of the bacteria. Therefore the Peanut-shaped ZnO-NBs action on *B. subtilis* changes the cell wall morphology as well as its permeability, ultimately leading to the bacterial growth by its death.

Fig.11. Antimicrobial activities of ZnO-NBs prepared at different temperature ranges against Gram-positive (*Bacillus subtilis*).

Table 3. Antimicrobial activity of Peanut-shaped ZnO-NBs prepared at different temperature ranges; TEMP-I and TEMP-II, against *B. subtilis* (MTCC 121).

Sample	**Conc. (µg/ml)**	**Zone of Inhibition (mm)** *B. subtilis* **(MTCC 121)**
Peanut-shaped ZnO-NB (40±3°C) TEMP-I	250	12
	500	20
Peanut-shaped ZnO-NB (60±3°C) TEMP-II	250	13
	500	22
ZnO Powder	250	-
	500	17
Doxycycline	30 µg/disc	33

Conclusion

This paper described the synthesis and characterization of Peanut-shaped ZnO Nano bunches (ZnO-NBs) by a simple *mechano-solution method* at various low temperatures range (TEMP-1 and TEMP-II). The effect of these temperatures on the particle size, morphology and L/D dimensions were reported. The SEM results presented the existence of Peanut-shaped 1D single crystals and Nano-bunches of ZnO where the transition of Peanut-shaped ZnO to Rod-shaped ZnO (on coming more down the process temperature line) occurs. The average crystallite size of ZnO-NB were observed as 66.25 nm at TEMP-II (60±3 °C), contrary to the one reported at TEMP-I (40±3 °C) which was found to be as 80.38 nm. The aspect-ratio was the maximum at TEMP-I and decreased on moving toward TEMP-II. Finally, the growth order of the Peanut-shaped ZnO-NBs revealed that the growth rate was maximum towards [0 0 0 I] facets at TEMP-I (40±3 °C). The presence of $C_{19}H_{42}NBr$ complex (stabilizer) that binds more towards the facets <0 I Ī I> & <0 I Ī 0>, changes the free energy and slows the growth of these facets at TEMP-I. A significant absorbances of light in UV-Vis range by Peanut-shaped ZnO-NBs clearly exhibit that it can be used more efficiently as sunscreens, photocatalysts, cosmetics, etc. The model developed shows the linear trend of change in L/D ratios of Peanut-shaped ZnO-NBs along with temperature. With the increase in temperature, the peanut-shaped ZnO-NBs become more symmetric which is appealing in many applications. In addition to all, the synthesized peanut-shaped ZnO- NBs also showed significant antimicrobial activity suggesting that peanut-shaped ZnO-NBs can be better agents to control the spreading of bacterial infections. Though *B. subtilis* is not as much harmful as other pathogenic bacterias, but it is an easy model for doing the clinical studies and checking the anti-bacterial activity, as the mechanism for attacking on the Gram +ve bacterial colonies are same. Therefore, we can postulate that our synthesized peanut-shaped ZnO-NBs may be externally used in a variety of therapeutic formulations as it is treated for potential interventions in extrinsic skin problems like aging, sunburn, etc.

Acknowledgement

The authors are thankful to the Department of Science & Technology (DST), under the scheme NANOMISSION, Ministry of Science & Technology, Government of India, New Delhi, India (Project No – SR/NM/NS/91-2008) for their financial support. The authors are also grateful to Dr. Ejaz Ahmad, Interdisciplinary Biotechnology Unit, Aligarh Muslim University, Aligarh. The authors are also thankful to the Advanced Materials Research Chair, KSU, Riyadh, Saudi Arabia.

References

[1] Ü. Özgür, Ya. I. Alivov, C. Liu, A. Teke, M.A. Reshchikov, S. Doğan, V. Avrutin, S.-J. Cho, H. Morkoç, A comprehensive review of ZnO materials and devices, J. App. Phy. 98 (2005) 041301.

[2] K. Rekha, M. Nirmala, Manjula G. Nair, A. Anukaliani, Structural, optical, photocatalytic and antibacterial activity of zinc oxide and manganese doped zinc oxide nanoparticles, Physica B, 405 (2010) 3180-3185.

[3] S.E. Cross, B. Innes, M.S. Roberts, T. Tsuzuki, T.A. Robertson, P. McCormick, Human Skin Penetration of Sunscreen Nanoparticles: In-vitro Assessment of a Novel Micronized Zinc Oxide Formulation, Skin Pharmacol Physiol, 20 (2007) 148-154.

[4] D. Nipane, S.R. Thakare, N.T. Khati, ZnO Nanoparticle By Sol-Gel And Its UV Application In Cosmetics Formulation, International Journal of Knowledge Engineering, 3(1) (2012) 168-169.

[5] J.G. Ionescu, The photoaging of human skin, in medicine, anti aging for professionals 2 (2005).

[6] A. Becheri, M. Dürr, P. Lo Nostro, P. Baglioni, Synthesis and characterization of zinc oxide nanoparticles: application to textiles as UV-absorbers, J. Nanopart. Res. 10 ((2008) 679-689.

[7] R. Wahab, Y.-S. Kim, H.-S. Shin, Effect of Refluxing Time on the Morphology of Pencil like Zinc Oxide Nanostructures Prepared by Solution Method, Met. Mater. Int. 16(5) (2010) 767-772.

[8] Y. Gan, F. Gu, D. Han, Z.Wang, G. Guo, Biomimetic Synthesis of Zinc Oxide 3D Architectures with Gelatin as Matrix, Journal of Nanomaterials, Article ID 289173(2010) 7 pages.

[9] S.G. Ansari, R.Wahab, Z.A. Ansari, Y.-S. Kim, G. Khang, A. Al-Hajry, H.-S. Shin, Effect of nanostructure on the urea sensing properties of sol–gel synthesized ZnO, Sens. Actuators, B 137 (2009) 566-573.

[10] J. Lu, K.M. Ng, S.H. Yang, Efficient, One-Step Mechanochemical Process for the Synthesis of ZnO Nanoparticles, Ind. Eng. Chem. Res. 47 (2008) 1095-1101.

[11] Wen-Yang Chang, Te-Hua Fang, Cheng-I Weng and Shin-Shing Yang, Flexible piezoelectric harvesting based on epitaxial growth of ZnO, Appl. Phys. A 102 (2011) 705-711.

[12] A. Mclaren, T. Valdes-Solis, G. Li, S.C.Tsang, Shape and Size Effects of ZnO Nanocrystals on Photocatalytic Activity, JACS 131 (2009) 12540-12541.

[13] R. Wahab, S.G. Ansari, Y.S. Kim, M. Song, H.-S. Shin, The role of pH variation on the growth of zinc oxide nanostructures, Appl. Surf. Sci. 255 (2009) 4891-4896.

[14] A.S. Ratkovich, R. Lee Penn, Controlling Nanosized ZnO Growth Kinetics Using Various Zn:OH Concentration Ratios, J. Phys. Chem. C 111 (2007) 14098-14104.

[15] A.S. Ratkovich, R.L. Penn, Controlling oriented aggregation using increasing reagent concentrations and trihalo acetic acid surfactants, J. Solid State Chem. 181 (2008) 1600-1608.

[16] H. Xue, X.L. Xu, Y. Chen, G.H. Zhang, S.Y. Ma, Influence of Ag-doping on the optical properties of ZnO films, Appl. Surf. Sci. 255 (2008) 1806-1810.

[17] K. Rekha, M. Nirmala, Manjula G. Nair, A. Anukaliani, Structural, optical, photocatalytic and antibacterial activity of zinc oxide and manganese doped zinc oxide nanoparticles, Physica B 405 (2010) 3180-3185.

[18] J. Xu, Q. Pan, Y. Shun, Z. Tian, Grain size control and gas sensing properties of ZnO gas sensor, Sens. Actuators, B 66 (2000) 277-279.

[19] Z. Qin, G. Zhang, Q. Liao, Y. Qiu, Y. Huang, Y. Zhang, Influences of low temperature thermal treatment on ZnO nanowire arrays and nanoparticles based flexible dye-sensitized solar cells, Colloids Surf., A 402 (2012) 127-131.

[20] R. Wahab, S.G. Ansari, Y.-S. Kim, H.-K. Seo, H.-S. Shin, Room temperature synthesis of needle-shaped ZnO nanorods via sonochemical method, Appl. Surf. Sci. 253 (2007) 7622-7626.

[21] R. Teki, T.C. Parker, H. Li, N. Koratkar, T.-M. Lu, S. Lee, Low temperature synthesis of single crystalline ZnO nanorods by oblique angle deposition, Thin Solid Films 516 (2008) 4993-4996.

[22] M. F. Khan, A.H. Ansari, E. Ahmad, Indian Patent Office, Application No. 219/DEL/2013 (2013).

[23] K. Rekha, M. Nirmala, Manjula G. Nair, A. Anukaliani, Structural, optical, photocatalytic and antibacterial activity of zinc oxide and manganese doped zinc oxide nanoparticles, Physica B 405 (2010) 3180-3185.

[24] D.C. Little, J. Dolovich, Respiratory disease in industry due to B. subtilis enzyme preparations, Can. Med. Assoc. J. 108(9) (1973) 1120-1125.

[25] C. Apetroaie-Constantin, R. Mikkola, M.A. Andersson, V. Teplova, I. Suominen, T. Johansson, M. Salkinoja-Salonen, Bacillus subtilis and B. mojavensis strains connected to food poisoning produce the heat stable toxin amylopsin, J. Appl. Microbiol. 106 (2009) 1976-1985.

[26] H.P. Bais, R. Fall, J.M. Vivanco, Biocontrol of Bacillus subtilis against Infection of Arabidopsis Roots by Pseudomonas syringae Is Facilitated by Biofilm Formation and Surfactin Production, Plant Physiol. 134 (2004) 307-319.

[27] J. Xie, P. Li, Y. Wang, Y. Wei, Synthesis of needle and flower-like ZnO microstructures by a simple aqueous solution route, J. Phys. Chem. Solids 70 (2009) 112-116.

[28] D. Cullity, Elements of X-ray Diffraction, Addition-Wesley Publishing Company Inc., USA, 1978.

[29] A.K. Singh, V. Viswanath, V.C. Janu, Synthesis, effect of capping agents, structural, optical and photoluminescence properties of ZnO nanoparticles, J. Lumin. 129 (2009) 874-878.

[30] L. Weinstein, C.G. Colburn, Bacillus Subtilis Meningitis And Bacteraemia Report of a Case and Review of the Literature On "Subtilis" Infections in Man, AMA Arch Intern Med., 86(4) (1950) 585-594. (doi:10.1001/archinte.1950.00230160097009)

[31] J.T. Seil, T.J. Webster, Antimicrobial applications of nanotechnology: methods and literature, Int. J. Nanomed. 7 (2012) 2767-2781.

[32] P.S. Hale, L.M. Maddox, J.G. Shapter, N.H.Voelcke, M.J. Ford, E.R. Waclawik, Growth Kinetics and Modeling of ZnO Nanoparticles, J. Chem. Educ. 82 (2005) 775.

[33] X.H. Guan, G.S. Wang, C.P. Li, Y.Z. Lv, L. Guo, H.B. Xu, Synthesis and optical properties of ZnO multipod nanorods, J. Lumin. 122–123 (2007) 770-772.

[34] N.R. Yogamalar, A.C. Bose, Tuning the aspect ratio of hydrothermally grown ZnO by choice of precursor, J. Solid State Chem. 184 (2011) 12-20.

[35] N. Jones, B. Ray, K.T. Ranjit, A.C. Manna, Antibacterial activity of ZnO nanoparticle suspensions on a broad spectrum of microorganisms, FEMS Microbiol. Lett. 279 (2008) 71-76.

[36] B.H. Sonia, M.P. Deshpande, S. V. Bhatta , S.H. Chakia, H. Kaheria, Study on antimicrobial activity of undoped and Mn doped ZnO nanoparticles synthesized by microwave irradiation, Archives of Applied Science Research, 3(6) (2011) 173-179.

[37] K.R. Raghupathi, R.T. Koodali, A.C. Manna, Size-Dependent Bacterial Growth Inhibition and Mechanism of Antibacterial Activity of Zinc Oxide Nanoparticles, Langmuir 27 (2011) 4020-4028.